COOPERATIVE VEHICLE MERGING ON HIGHWAYS – MODEL PREDICTIVE CONTROL

Ioannis A. Ntousakis
School of Production Engineering and Management
Technical University of Crete, University Campus, GR-73100, Chania, Greece
Email: intousakis@dssl.tuc.gr

Ioannis K. Nikolos, Corresponding Author
School of Production Engineering and Management
Technical University of Crete, University Campus, GR-73100, Chania, Greece
Tel: +30-2821037300; Email: jnikolo@dpem.tuc.gr

Markos Papageorgiou
School of Production Engineering and Management
Technical University of Crete, University Campus, GR-73100, Chania, Greece
Tel: +30-2821037240; Email: markos@dssl.tuc.gr

Word count: 5,745 words text + 7 tables/figures x 250 words (each) = 7,495 words

Submission Date: November 9th, 2016

ABSTRACT

The problem of trajectory planning for the cooperative merging of vehicles in highways was previously formulated by the authors as a finite-horizon optimal control problem and was solved analytically. In this work, the trajectory planning approach is further extended in various respects, and an alternative solution procedure via a time-variant Linear-Quadratic Regulator approach is also presented. Most importantly, a Model Predictive Control (MPC) scheme is utilized to compensate possible disturbances in the trajectories of the cooperating vehicles, whereby the analytical optimal solution is applied repeatedly in real time, using updated measurements, until the merging procedure is actually finalized. The methodology is demonstrated for a set of vehicles inside the merging area. Various numerical simulations illustrate the validity and applicability of the method.

Keywords: Optimal vehicle trajectory planning, Cooperative merging, Automated vehicles, Connected vehicles, Model Predictive Control

1. INTRODUCTION

The merging of mainstream traffic flow with the incoming flow at on-ramps is a serious source of traffic flow problems on highways (*1*), (*2*), (*3*), (*4*), (*5*). As the interacting vehicles and drivers in the merging procedure have different abilities and characteristics, the merging process is often performed inefficiently with respect to the traffic flow, passengers' safety and comfort. To address these issues, an increasing effort has been spent for the development of merging assistance and control systems that enable cooperative merging of equipped vehicles (*2*). Typically, the overall merging control problem is decomposed into: (a) The computation of a merging sequence (MS) for approaching vehicles on the mainstream and the on-ramp as the task of an upper-level controller; and (b) the appropriatewhile the lower-level merging controller is dedicated to the merging maneuvers of the involved vehicles via a lower-level merging controller. The merging problem was formulated as an optimal control problem in (*6*) for a given merging sequence; several works have been published thereafter for the creation of the merging sequence, see the references in (*7*).

The lower-level controller has typically two tasks: the creation of the proper gaps for subsequently merging vehicles, and the control of individual vehicles to produce an efficient and safe merging (*2*). These tasks should be arranged so as to minimize conflicts in the merging region and limit speed changes. Various approaches to address these tasks have been proposed, e.g. in (*1*), (*3*), (*6*), (*7*), (*8*), (*9*), (*10*), (*11*); see (*7*) and (*12*) for more detailed literature review and discussion.

A trajectory planning methodology is developed and presented in (*12*), to enable automated merging of single-lane mainstream and single-lane on-ramp vehicles. The designed trajectories minimize the engine effort and passenger discomfort by minimizing vehicle acceleration, jerk and its first derivative. The proposed methodology in (*12*) may enable efficient merging by ensuring pre-specified time-headways and vehicle speeds at the end of the maneuver, corresponding to maximum throughput. To this end, a finite-horizon optimal control problem with fixed final states is formulated, and solved analytically. Tunable weights are used in (*12*) for combining the different optimization sub-criteria.

A Model Predictive Control scheme is established to compensate possible disturbances in the trajectories of the merging vehicles, by using updated real-time measurements in each time step for the formation of the remaining part of the optimal trajectory; then, the methodology is further developed and tested for a set of vehicles inside the merging area. The paper is structured as follows: in Section 2 the overall merging control framework is presented in brief. In Section 3, a discrete-time Quadratic Programming formulation, which allows for explicit consideration of inequality constraints, as well as an alternative solution procedure via a time-variant LQR (Linear-Quadratic Regulator) approach are offered; also, the lateral movement of on-ramp vehicles is addressed. In Section 4, the MPC framework is presented and applied to specific examples; furthermore, it is compared to a typical ACC-based merging system. Subsequently, the MPC framework is further generalized for a set of vehicles. The concluding remarks are presented in Section 5.

2. THE MERGING CONTROL FRAMEWORK

A single mainstream motorway lane with a single-lane on-ramp leading to an acceleration lane is considered, as illustrated in Figure 1 (Top), with the fixed merging point close to the end of the acceleration lane. A cooperation area is defined, starting from a pre-specified distance upstream of the merging point and ending at the merging point. The use of a fixed merging point allows for the longitudinal and lateral movements of vehicles to be treated independently. For the longitudinal movement, the position of each vehicle inside the cooperation area is defined by its lane (mainstream or on-ramp) and its x-distance from the merging point. In the following, when addressing a specific merging vehicle, we will call it the ego vehicle. It is assumed that an upper control level exists, which performs the determination and update of the Merging Sequence (MS) according to appropriate criteria. A given MS implies that, for each vehicle inside the cooperation area, a "putative leader" (i.e. the preceding vehicle in the MS) has been assigned (Figure 1 (Middle)), and this is actually the output of the upper control level. The putative leader of a vehicle may or may not be its physical leader, as it can be a vehicle of a different lane.

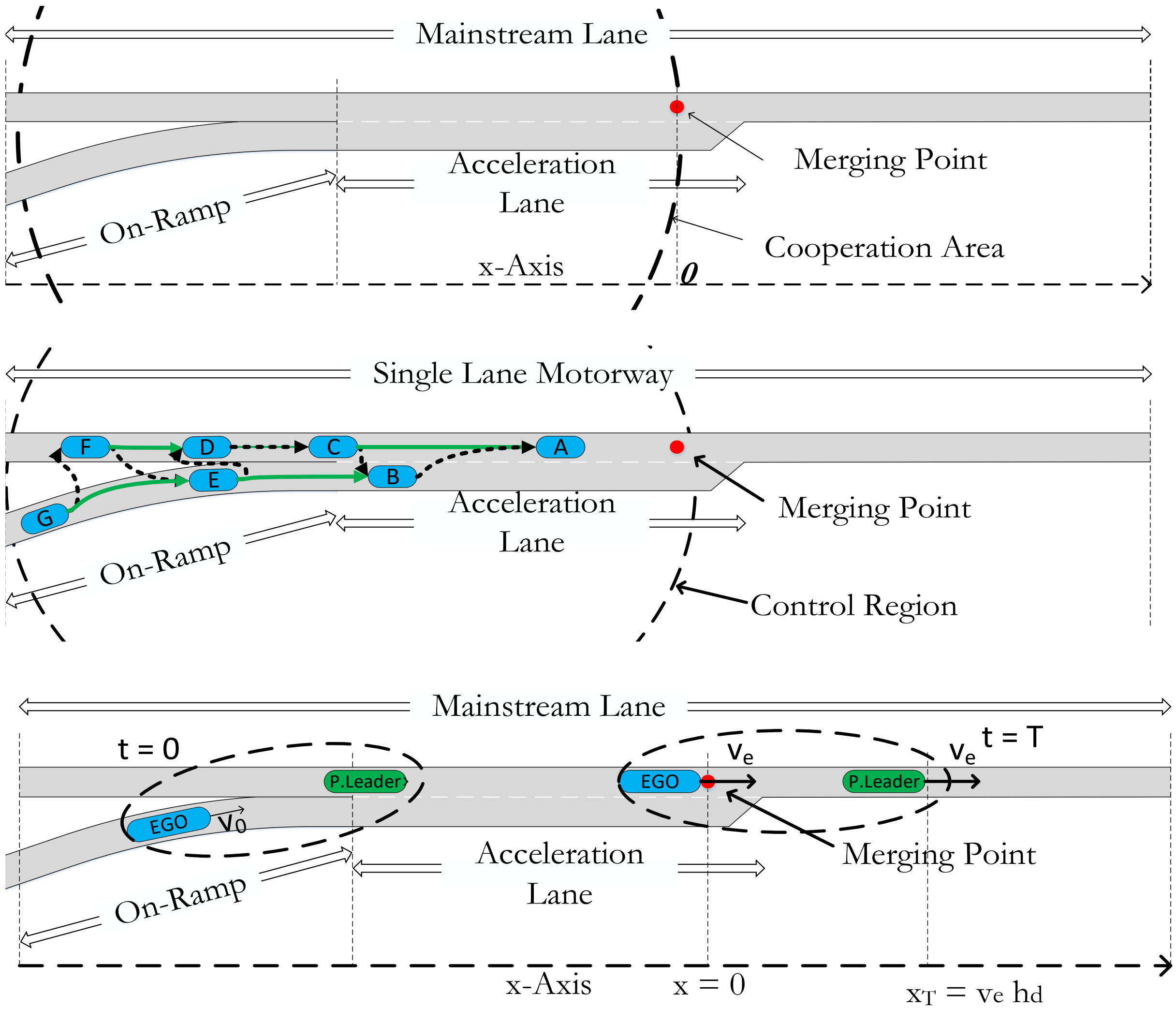

FIGURE 1 (Top) The topology of the motorway.
(Middle) For each vehicle in the cooperation area, the green solid arrow indicates its physical leader and the dashed black arrow the putative leader.
(Bottom) Positions of the ego vehicle and its putative leader.

To implement the MS, merging trajectories are produced to guide the individual vehicle movement from its current state (position and speed) to the merging point (Figure 1 (Middle)). We will specify here that the merging trajectory of each controlled vehicle should feature a (final) speed equal to the final speed of its putative leader, and a final time-headway to its leader equal to the pre-specified one (set by the driver of the merging vehicle on the on-board (C)ACC system) (Figure 1 (Bottom)); other, e.g. throughput maximizing choices may be found in (*12*). When the merging trajectory of the ego vehicle is computed and continuously updated in real time, its putative leader may not have reached the merging point yet. However, based on the putative leader's own computations, an estimated final merging time and speed is available, which can be communicated to the ego vehicle. Thus, the desired final speed v_e of the ego vehicle at the merging point can be estimated and updated.

The trajectory planner presented in (*12*) optimizes a combined cost function, which takes into account (with appropriate weights) the acceleration a, the jerk j, and the time-derivative of the jerk d of the merging vehicle. The system is described with four state equations and the objective is to bring the system from its initial condition $\boldsymbol{x_0} = \left[x_0\ v_0\ a_0\ j_0\right]^{\mathrm{T}}$ to the final condition $\boldsymbol{x_e} = \left[0\ v_e\ 0\ 0\right]^{\mathrm{T}}$ by time T at the merging point, assuming that each merging vehicle knows its final speed (v_e) and time of arrival at the merging point (T) beforehand. The solution is derived analytically and calls for the online solution of a linear system of eight equations reflecting the initial and final conditions, see (*12*) for details.

3. EXTENSIONS TO VEHICLE MERGING TRAJECTORY PLANNING

3.1 Discrete-time formulation

The continuous-time optimal control problem may also be formulated in discrete time, in which case the resulting optimization may be cast in the form of a Quadratic Programming (QP) problem (*13*). Let τ be the discrete time step. Let $a_k = a(k\tau), j_k = j(k\tau), d_k = d(k\tau)$ be the acceleration, the jerk, and the time derivative of jerk, respectively, at discrete time instants $k = 0,1,2, \dots K$, with $K = T/\tau$ being the total number of discrete time steps (time horizon). Then the cost function to be minimized is

$$Z = \sum_{k=0}^{K-1} (w_1 a_k^2 + w_2 j_k^2 + d_k^2). \qquad (1)$$

Similarly, we define with x_k and v_k the position and speed of the vehicle at time instant k. Assuming a constant value of the (virtual) control variable d_k during each time step $[k\tau, (k + 1)\tau)$, the state variables obey the following linear discrete-time state equations:

$$x_{k+1} = x_k + v_k\tau + \frac{1}{2}a_k\tau^2 + \frac{1}{6}j_k\tau^3 + \frac{1}{24}d_k\tau^4 \qquad (2)$$

$$v_{k+1} = v_k + a_k\tau + \frac{1}{2}j_k\tau^2 + \frac{1}{6}d_k\tau^3 \qquad (3)$$

$$a_{k+1} = a_k + j_k\tau + \frac{1}{2}d_k\tau^2 \qquad (4)$$

$$j_{k+1} = j_k + d_k\tau \qquad (5)$$

with the following initial and final conditions:

$$
\begin{aligned}
&x_0 = x(0)\ , x_K = x(K) = 0 \\
&v_0 = v(0), v_K = v(K) \\
&a_0 = a(0), a_K = a(K) = 0 \\
&j_0 = j(0),\ j_K = j(K) = 0.
\end{aligned}
\tag{6}
$$

The only difference of this discrete-time optimal control problem from its continuous-time counterpart in (*12*) is due to the fact that the (virtual) control variable d_k is constant for the duration of each time period τ. Hence, the solution of both problems will be virtually identical for sufficiently small τ. Despite the impressive recent advancements with solution codes for QP control problems (*14*), the formulation of the merging trajectory design problem in QP format is not expected to provide computational advantages over the reported analytical solutions in (*12*); its potential advantage is that it allows for incorporation of inequality constraints in the optimal control problem.

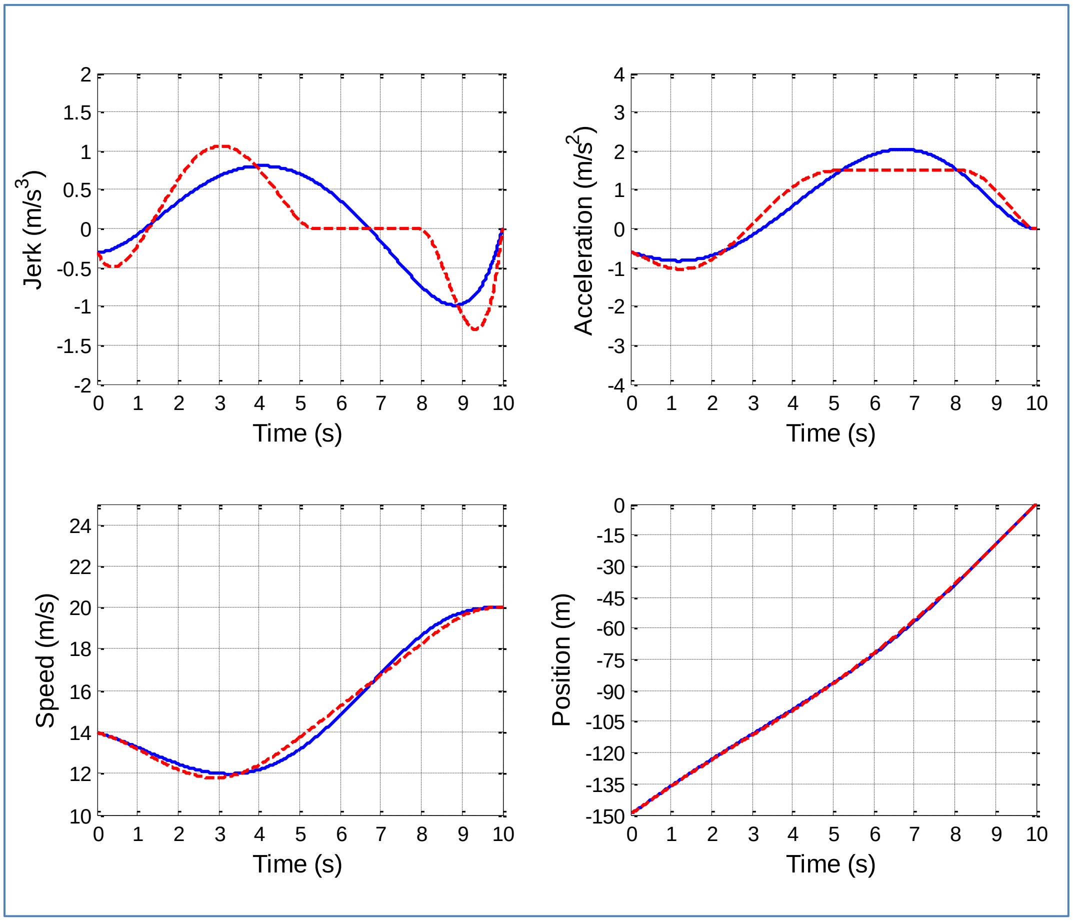

FIGURE 2 Graphical representation of the resulting optimal solutions using QP, for the case with $x_0 = -150\ m, x_e = 0\ m, v_0 = 14\frac{m}{s}, v_e = 20\frac{m}{s},\ a_0 = -0.6\frac{m}{s^2}, a_e = 0\ \frac{m}{s^2},\ j_0 = -0.3\frac{m}{s^3},\ j_e = 0\frac{m}{s^3}, T = 10\ s$; solid blue line: no constraints are activated; dashed red line: imposed maximum acceleration $a_{max} = 1.5\frac{m}{s^2}$.

3.2 QP formulation with inequality constraints

The QP formulation can be used to compute the optimal solution in the case where constraints are also imposed for the maximum and minimum permissible values of the state variables. This is demonstrated in the following example, referring to the case with the combined cost function (Equation (1)), with the following initial and final conditios: $x_0 = -150\ m, x_e = 0\ m, v_0 = 14\frac{m}{s}, v_e = 20\frac{m}{s}, a_0 = -0.6\frac{m}{s^2}, a_e = 0.0\frac{m}{s^2}, j_0 = -0.3\frac{m}{s^3}, j_e = 0\frac{m}{s^3}, T = 10\ s$, and weights $w_1 = 0.1, w_2 = 0.5$. The optimal solution for the unconstrained case is visible in Figure 2, along with the resulting optimal solution when a maximum value in acceleration equal to $a_{max} = 1.5\frac{m}{s^2}$ is imposed. The optimal solution is accordingly modified to satisfy the imposed constraint, resulting in steeper variations of jerk outside the region where the constraint is activated, in order to fulfil the initial and final conditions.

3.3 Time-varying LQR (Linear-Quadratic Regulator) formulation

The unconstrained optimal control problem, for the continuous-time (analyzed in (*12*)) or the discrete-time formulation (Section 3.1), is a Linear Quadratic (LQ) one, since the system state is described by a set of linear differential or difference equations, while the cost function is of quadratic form. Thus, the solution of this problem can be given in linear feedback form, as a linear-quadratic-regulator (LQR). The LQR may be developed in very similar ways in either continuous time or discrete time. In the following, the discrete-time LQR derivation is presented for the problem under consideration.

Equations (2)-(5) constitute a discrete-time linear system which may be expressed in state-space form

$$\boldsymbol{x_{k+1}} = \boldsymbol{A} \cdot \boldsymbol{x}_k + \boldsymbol{b} \cdot u_k \tag{7}$$

where $\boldsymbol{x} = [x\ v\ a\ j]^{\mathrm{T}}$ is the state vector and $u = d$ is the (virtual) control input. The quadratic performance index (Equation (1)) is extended with a final-time term

$$J = \frac{1}{2}\|\boldsymbol{x}_K\|_{\boldsymbol{S}}^2 + \frac{1}{2}\sum_{k=0}^{K-1}\left[\|\boldsymbol{x}_k\|_{\boldsymbol{Q}}^2 \quad + u_k^2\right]. \tag{8}$$

As in Equation (1), we have the diagonal state-weighting matrix $\boldsymbol{Q} = diag(0\ 0\ w_1\ w_2)$. The final-time term is introduced to guarantee that all final states $\boldsymbol{x}_K$ will be virtually zero; to this end, the elements of the diagonal weighting matrix $\boldsymbol{S}$ are chosen sufficiently high. It can be shown (*13*) that the optimal control sequence minimizing the performance index is delivered by the linear feedback law

$$u_k = -\boldsymbol{L}_k \cdot \boldsymbol{x}_k \tag{9}$$

where $\boldsymbol{L}$ is the time-varying feedback gain vector, which may be computed via the following equations

$$\boldsymbol{L}_k = [\boldsymbol{b}^{\mathrm{T}}\boldsymbol{P}_{k+1}\boldsymbol{b} + 1]^{-1}[\boldsymbol{b}^{\mathrm{T}}\boldsymbol{P}_k\boldsymbol{A}] \tag{10}$$

$$\boldsymbol{P}_k = \boldsymbol{A}^{\mathrm{T}}\boldsymbol{P}_{k+1}\boldsymbol{A} + \boldsymbol{Q} - \boldsymbol{L}_k^{\mathrm{T}}\boldsymbol{b}^{\mathrm{T}}\boldsymbol{P}_{k+1}\boldsymbol{A} \tag{11}$$

with terminal condition

$$\boldsymbol{P}_K = \boldsymbol{S}. \tag{12}$$

The matrix $\boldsymbol{P}_k$ is referred to as the discrete-time Riccati matrix and it can be computed, along with the gain $\boldsymbol{L}_k$, through backward integration, starting from Equation (12) and utilizing Equations (10) and (11).

The above feedback control law will drive the system to the origin ($\boldsymbol{x}_K = 0$) in final time K from any initial state $\boldsymbol{x}(0) = \boldsymbol{x}_0$. In our case however, we need all final states to be driven to the origin, except for the speed, which should be driven towards the desired final speed v_e. For this reason, the problem must be reformulated such that all states are driven to zero. To this end, we introduce the variable v^* as

$$v_k^* = v_k - v_e. \tag{13}$$

Equation (2) for the position now becomes

$$x_{k+1} = x_k + v_k^*\tau + \frac{1}{2}a_k\tau^2 + \frac{1}{6}j_k\tau^3 + \frac{1}{24}d_k\tau^4 + v_e\tau. \tag{14}$$

Accordingly, Equation (3) for the speed becomes

$$v_{k+1}^* = v_k^* + a_k\tau + \tfrac{1}{2}j_k\tau^2 + \tfrac{1}{6}d_k\tau^3. \tag{15}$$

The remaining system equations (acceleration and jerk) remain unchanged. The new equations may be written in state-space form

$$\boldsymbol{x}_{\boldsymbol{k+1}} = \boldsymbol{A}\cdot\boldsymbol{x}_k + \boldsymbol{b}\cdot u_k + \boldsymbol{\delta} \tag{16}$$

where now $\boldsymbol{x} = [x\ v^*\ a\ j]^{\mathrm{T}}$ and the vector $\boldsymbol{\delta} = [v_e\tau\ 0\ 0\ 0]^{\mathrm{T}}$ acts as a constant and known disturbance to the system. In this case, the optimal control law is extended (*15*) as

$$u_k = -\boldsymbol{L}_k\boldsymbol{x}_k - U_k \tag{17}$$

For computing the feedforward term U_k, we use the following definitions:

$$\boldsymbol{D}_k = [1 + \boldsymbol{b}^{\mathrm{T}}\boldsymbol{P}_{k+1}\boldsymbol{b}]^{-1}\boldsymbol{b}^{T} \tag{18}$$

$$\boldsymbol{Z}_k = \boldsymbol{A}^{\mathrm{T}}[\boldsymbol{I} - \boldsymbol{P}_{k+1}\boldsymbol{b}\boldsymbol{D}_k] \tag{19}$$

$$\boldsymbol{p}_K = \boldsymbol{P}_K\boldsymbol{\delta} \tag{20}$$

$$\boldsymbol{p}_k = \boldsymbol{P}_k\boldsymbol{\delta} + \boldsymbol{Z}_k\boldsymbol{p}_{k+1} \tag{21}$$

The vector $\boldsymbol{p}_k$ can be computed using Equations (18-21). Finally we have $U_k = \boldsymbol{D}_k\boldsymbol{p}_{k+1}$. It is important to note that the matrices $\boldsymbol{P}_k$ and $\boldsymbol{L}_k$ can be computed offline only once, for a sufficiently long K, and be stored inside the vehicle, since they depend only on the a priori known matrices $\boldsymbol{A}, \boldsymbol{b}, \boldsymbol{Q}$; while the feedforward term U_k depends also on the desired final speed (v_e) and must therefore be computed online (or be stored for a range of different final speeds). The LQR solution is virtually equivalent to the analytical solution derived in (*12*), but it might present computational advantages. In particular, the feedback control law in Equation (17) is by itself equivalent to an MPC procedure, because it is not dependent on any particular initial state.

2.4 Lateral Movement

For the final merging of vehicles stemming from the on-ramp, a lateral lane change from the acceleration lane to the mainstream lane is of course necessary. All previous developments did not address explicitly this lateral part of the on-ramp merging vehicle trajectory. This is because the presence of a fixed merging point (Figure 1 (Top)) allows for an independent design of the lateral vehicle movement. Specifically, on-ramp merging vehicles need to move, short before reaching the merging point, in lateral direction from an initial position $y(0) = -\Delta$, Δ being the lane width, to zero. The time period for the execution of the lane change maneuver may be pre-specified to be either constant (few seconds) or dependent on the desired longitudinal merging speed v_e. The initial speed, acceleration and jerk in lateral direction at the start of the maneuver are obviously all equal to zero; while the respective final values at the end of the maneuver should also be all equal to zero. The state equations and objective criterion for the lateral movement are the same as for the longitudinal movement in previous sections. However, since the final values of all lateral state variables must be equal to zero, the ordinary LQR (Equation (9)) with offline computed gain matrix may be employed online for the lateral movement with very low computation requirements.

4. APPLICATION OF A MODEL PREDICTIVE CONTROL FRAMEWORK

4.1 The Necessity of MPC

In the previous developments we adopted the assumption that each merging vehicle knows its final speed (v_e) and time of arrival at the merging point (T) beforehand, while computing its trajectory. However, these values may be subject to modifications as the vehicle is moving in an actual merging scenario for several reasons. In order to tackle such real-time changes, which call for corresponding updates of the vehicle trajectory, a Model Predictive Control (MPC) scheme is utilized. In this way, possible disturbances in the trajectories of the merging vehicle and its putative leader can be compensated, as the optimization problem is repeatedly solved (or the LQR is applied in real time), using the updated data for the formation of the remaining part of the optimal trajectory. Thanks to the pursued problem formulation, the optimal solution's general form remains always the same (in every time step); what changes are only the initial state, the remaining time horizon and, possibly, the final merging speed. Thus, the solution constants can be re-calculated as functions of the initial conditions, as well as of v_e and T; or the LQR (Equation (17)) may be simply activated, possibly with an update of the feedforward term, in case of final speed change. This procedure is repeated regularly, e.g. each second; until the vehicle merging has been actually accomplished.

4.2 MPC Application Examples

We assume in this section that the putative leader can transmit only its current speed and position to the ego vehicle. Therefore, it is necessary to make an assumption regarding the future movement of the putative leader, which will enable the ego vehicle to estimate its expected time of arrival (T) and expected speed (v_e) and be able to apply the optimal control. The simplest assumption for estimating the aforementioned values is the one of constant speed for the remaining part of the trajectory of the putative leader. Clearly, this naïve assumption presents a challenge to the ego vehicle if the leader is actually changing its speed, hence the resulting merging control may, under circumstances, lead eventually to strong acceleration requirements. Under this naïve assumption, the putative leader will move at constant speed from the current time $t = t_0$ until the time $t = t_0 + T$. Consequently, the expected speed and expected time of arrival of the ego vehicle can be easily calculated as follows:

$$v_e = v_L(t_0) \tag{22}$$

$$T = \left|\frac{h_d \cdot v_e - x_L(t_0)}{v_L(t_0)}\right| = \left|h_d - \frac{x_L(t_0)}{v_L(t_0)}\right| \tag{23}$$

where the subscript "L" refers to the putative leader, with h_d being the desired headway setting of the ego vehicle. If, for any reason, the putative leader is stopped in the current time step (i.e. $v_L(t_0) = 0$), a suitable trajectory is applied to the ego vehicle, so as to have it stop at a safe distance behind the putative leader. In order to calculate this trajectory we set $v_e = 0$, while T is calculated from

$$T = \frac{v}{a_{comf}} \tag{24}$$

where α_{comf} is a comfortable deceleration. Also, since the optimal solutions are designed to satisfy the final condition $x(T) = 0$, the x-axis for this exceptional case should be suitably "shifted"; such that the new initial position to be used in the optimal solution calculation is $x' = x - \left(x_L - \left(l_L + r_{safe}\right)\right)$, where l_L is the length of the putative leader and r_{safe} is the safe distance.

In the first example (Figure 3 (Top)), the putative leader drives at a constant speed of 15 m/s; then it accelerates to 20 m/s; and continues thereafter at a constant speed. The ego vehicle assumes, at each MPC update, a constant future speed for its putative leader, equal to the leader's current speed. The simulation step is equal to 0.01s, while $w_1 = 0.1$, $w_2 = 0.5$. In Figure 3 (Top), different results of the MPC scheme are presented for different values of the MPC control step used (control step: blue=0.1 s, red=0.5 s, black=2.0 s). From Figure 3 (Top) it may be seen that the system works as expected, converging to the prescribed final speed and headway. However, by increasing the control intervals, the total cost is also increasing (Table 1 (Top)) because, in order to address the accumulated estimation error in cases of longer control steps, the ego vehicle needs to apply stronger maneuvers.

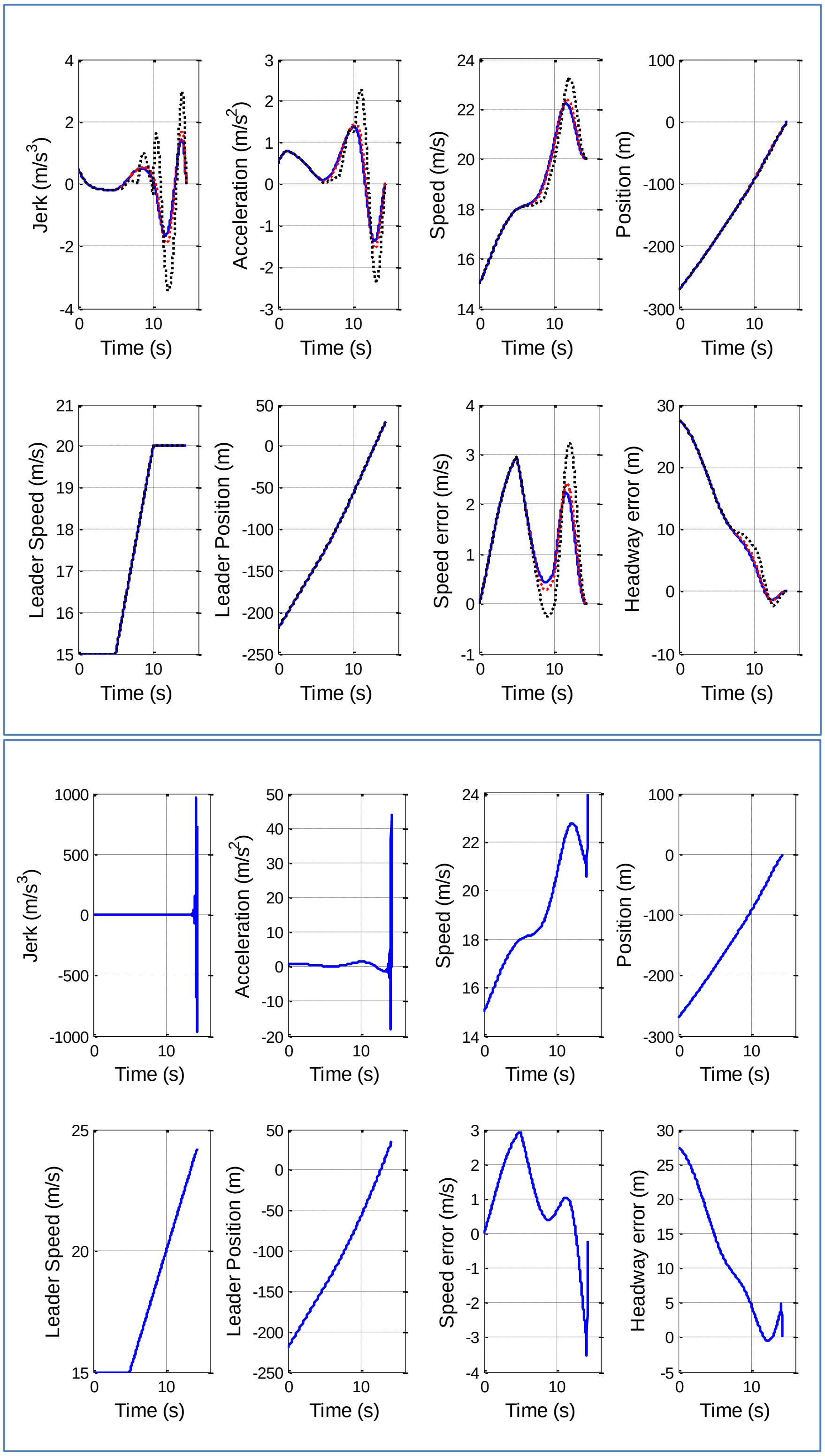

FIGURE 3 The effect of the control step on the resulting trajectory with the MPC, for the case when a constant speed is assumed for the putative leader. (Top) 1st scenario: the putative leader accelerates and then follows a constant speed trajectory (control step: blue=0.1 s, red=0.5 s, black=2.0 s). (Bottom) 2nd scenario: the putative leader accelerates until the merging point (control step: 0.2 s).

Simulations have been also performed for the case where the leader continues to accelerate throughout the duration of the merging process. This example was introduced to illustrate the difficulties that might arise in case of a naïve MPC prediction regarding the leader's speed. In such a case, there will always be a speed and headway error at the end of the merging maneuver, since the ego vehicle assumes constant leader speed, while the putative leader actually accelerates. Particularly, when the ego vehicle is close to the merging point, the remaining time is not sufficient to compensate for the error, and the optimal solution may impose large accelerations. This situation can be improved if the prediction regarding T and v_e can become more accurate (not using the assumption of constant speed for the remaining of the trajectory), or the putative leader can communicate its estimated final merging time and speed according to its own optimal trajectory planning. In order to visualize this problem, the example in Figure 3 (Bottom) is used. Note that, if hard inequality constraints (for acceleration and speed) would be considered here, this might render the optimization problem infeasible.

TABLE 1 (Top) The effect of the control step on the cost of the produced trajectory for the case of Figure 3 (Top).
(Bottom) The initial conditions for the vehicles involved in the test of Figure 5 (Bottom).

Control Step	0.1 s	0.2 s	0.5 s	1.0 s	2.0 s
Cost	17.3	18.7	24.1	38.4	101.4

Vehicle ID	**L**	**A**	**B**	**C**	**D**	**E**
Position (m)	-300	-330	-342.5	-360	-368	-390
Speed (m/s)	20	20	17	20	17	20
Acceleration (m/s^2)	0	0	0	0	0	0
Jerk (m/s^3)	0	0	0	0	0	0

4.3 Comparison with ACC-Controller Merging

In this section, the proposed method will be compared to a typical ACC controller (*16*) merging policy. As a matter of fact, several works have proposed the derivation of a merging trajectory for the ego vehicle by applying its ACC control law to a so-called "virtual" vehicle, which is basically a "projection" of the putative leader to the same lane as the ego vehicle (*7*), (*17*). Although this control method has the advantage that it does not need a separate controller to react to the putative leader's movement, it can lead to unnecessarily strong accelerations or decelerations. In the following, we use the same leader movement as in Figure 3 (Top) to test the reaction of the ACC merging controller and compare with the optimal control case.

The ACC controller used in this work is the following (*18*):

$$a_{des} = K_1(v_L - v) + K_2(x_L - x - v \cdot h_d) \tag{25}$$

where a_{des} is the desired acceleration and v is the speed of the ego vehicle, v_L is the speed of the leader, x is the position of the ego vehicle, x_L is the position of the leader, h_d is the desired time headway and K_1, K_2 are the control gains, with values 1.19 and 1.72, respectively. The desired acceleration is bounded by the maximum acceleration and the maximum deceleration, usually in the range between -4 to 3 m/s^2; moreover, the jerk was also bounded in the range between -3 and 4 m/s^3. The simulation step is equal to 0.01 s, while the control step equals 0.2 s. The produced trajectory using the ACC controller is presented in Figure 4. Other values for K_1, K_2 provided similar results (for example the ones proposed in (*18*) $K_1 = 1.7$, $K_2 = 1.12$,). It is evident that the merging procedure virtually nullifies the final speed and headway errors, but the produced trajectory features large and abrupt variations in acceleration and jerk, contrary to the smoother ones produced by the proposed methodology. The resulting value of the trajectory cost for ACC is significantly higher than in the optimal control case; however, the two costs are not directly comparable, as a) the ACC controller does not control jerk and its time derivative, while b) the optimal controller has not acceleration and jerk constraints.

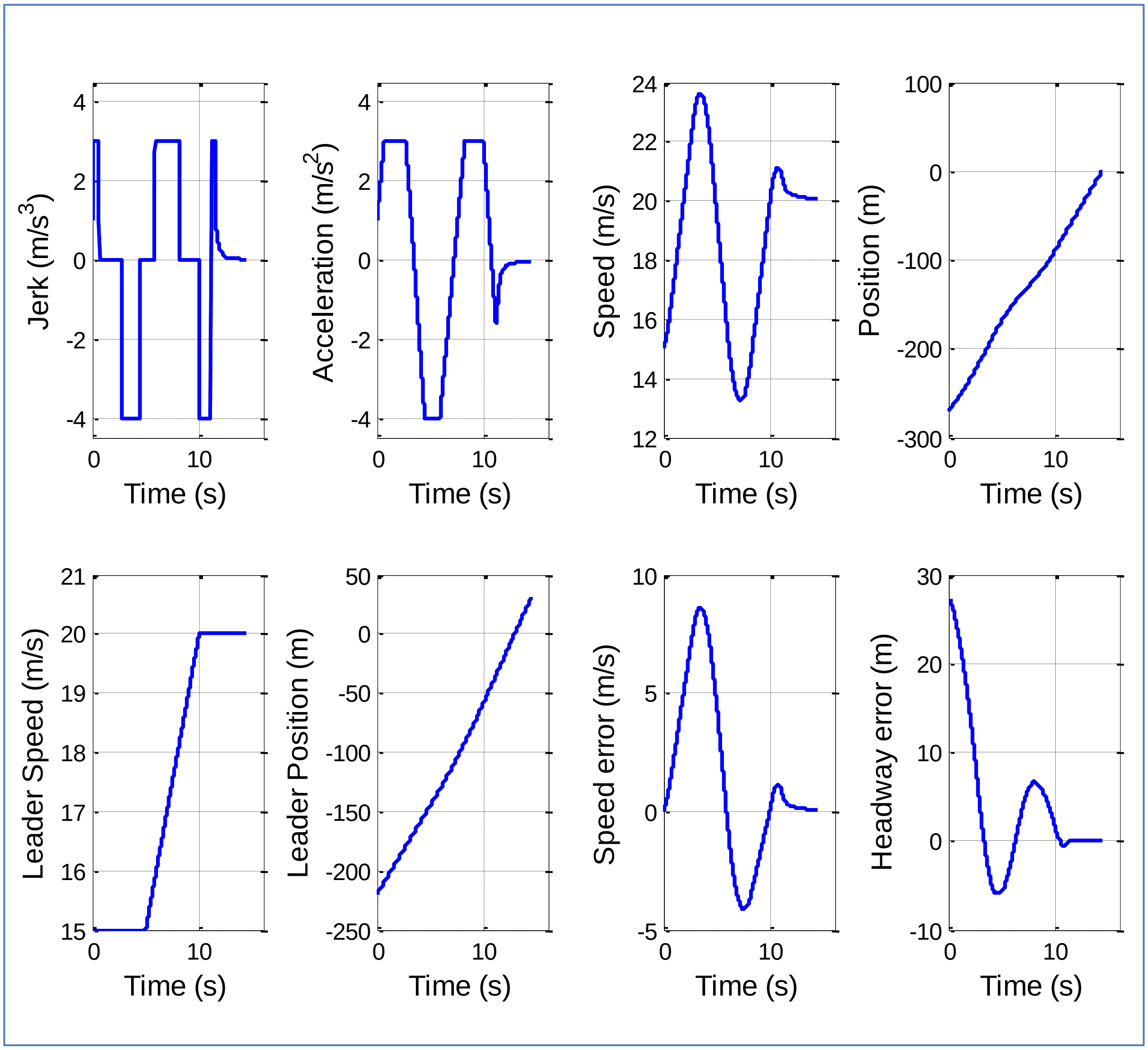

FIGURE 4 The produced trajectory using the ACC merging controller.

4.4 Application to a set of vehicles

In this section, a more general and ordinary application of the proposed methodology is presented; the effectiveness of the proposed methodology is assessed in a scenario where a set of several vehicles exists inside the cooperation area, and all of them follow the proposed methodology. In order to facilitate such a scenario, the following assumptions are adopted:

- An upper control level decides on the merging sequence of the vehicles inside the cooperation area and updates it on a regular basis, in order to deal with disturbances or other unexpected events.
- Each merging vehicle is equipped with a controller that applies the MPC scheme, as described in the previous sections, and computes an optimal trajectory.
- All vehicles are equipped with an ACC controller, which enables the automatic following of their leading vehicles in the same lane (actual leaders). Outside the cooperation area, only the ACC controller is active – for all vehicles.
- The MPC and ACC controllers are simultaneously active, inside the cooperation area, while the command that is actually applied to the vehicle is the most restrictive one. This is necessary in order to guarantee safety.
- No constraints are imposed in this work for the extreme values of jerk, acceleration, and speed (for both controllers - for compatibility reasons).
- The merging control process ends for a vehicle, once it has successfully merged into the mainstream.

Each merging vehicle, in order to be able to apply the proposed methodology, needs two values (at each control step): the expected time of arrival (T) and the expected speed v_e at the merging point, which are provided by its putative leader. Each putative leader continuously transmits the updated information to the corresponding follower vehicle until its merging, for updating the latter's optimal trajectory at every control step. A flow chart of the MPC methodology for a set of vehicles is presented in Figure 5 (Top).

In the following examples, an application of this methodology to a set of vehicles is presented, to demonstrate: a) its applicability and practicality, and b) how the variations in the movement of the putative leader affect the corresponding ego vehicle. As a demonstration example, we consider a set of 6 vehicles, initially travelling under ACC control, which enter the cooperation area successively (Figure 5 (Bottom)). The merging sequence for this example is pre-defined to be L-A-B-C-D-E (Figure 5 (Bottom)); however, in a real application this MS would be dynamically determined by the upper level controller. We assume that the cooperation area begins 200 m upstream of the merging point. The leading vehicle L is moving with a constant speed.

As previously mentioned, the movement of vehicles is affected by the merging system, only when they are located inside the cooperation area. For this experiment, it is assumed that any vehicle that has no actual and no putative leader travels with acceleration equal to zero. The simulation step was set equal to 0.1 s (same for the ACC controller step), while the control step for the MPC was set to 0.2 s. Table 1 (Bottom) contains the initial conditions for the vehicles involved in the test. The simulation results for the first example are depicted in Figure 6 (Top). Before commenting on the results of Figure 6 (Top), it should be emphasized that this particular example is a demanding one, since the mainstream vehicles arriving in the cooperation area have already the desired distance with their actual leaders (provided by the active ACC systems). However, in order to allow for the two on-ramp vehicles to merge, the necessary gaps should be created; thus, they need to perform a maneuver to first decelerate and, once the gaps are created, accelerate again to reach the speeds of their putative leaders. These maneuvers are automatically (and optimally) created by the proposed optimal control methodology. In the performed simulation (Figure 6 (Top)), the system proves capable to successfully implement the decision of the upper level controller regarding the merging sequence. In other words, the vehicles move on to the downstream section in the prescribed order. Equally importantly, the vehicles merge with the correct speeds and headways. Finally, the average accelerations imposed can be considered acceptable, although in some cases high instantaneous values were unavoidable.

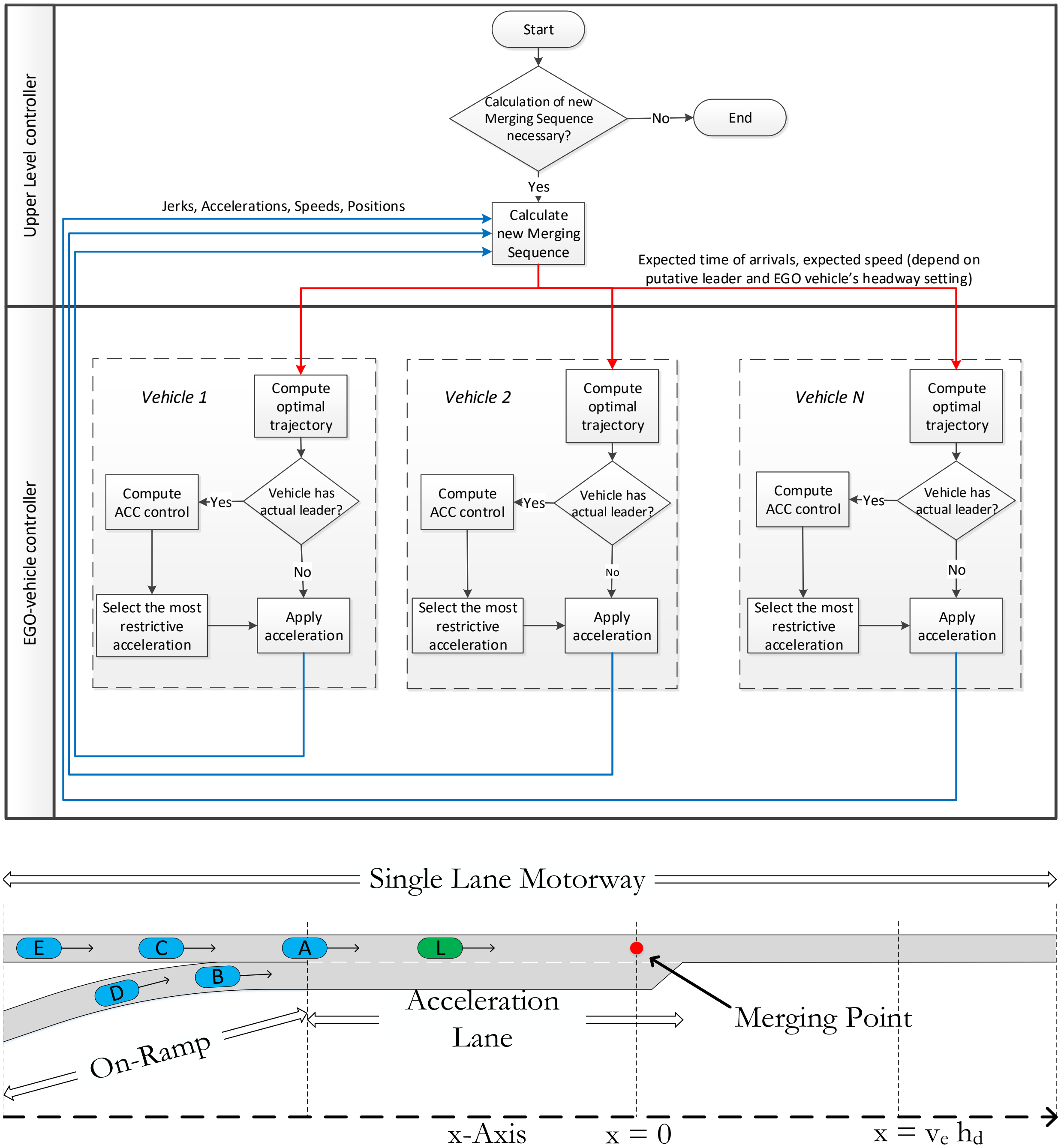

FIGURE 5 (Top) The flow chart of the MPC methodology applied for a set of vehicles. (Bottom) Representation of the predefined merging sequence for the set of vehicles involved in the automated merging procedure.

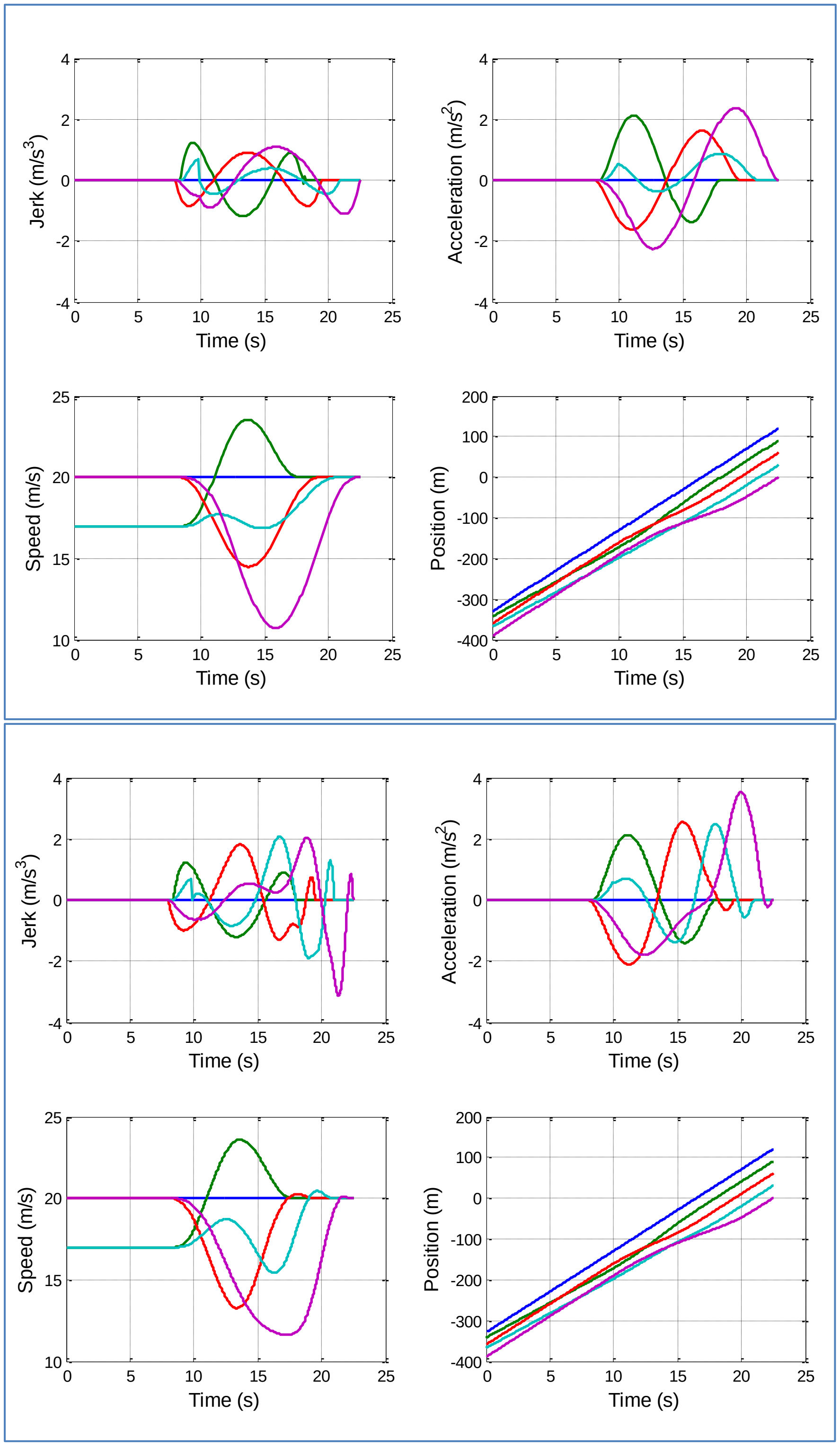

FIGURE 6 Application of the MPC scheme to a set of vehicles. (Top) 1st scenario: the putative leaders transmit their expected times and speeds at the merging point; vehicles: A: Blue, B: Green, C: Red, D: Light Blue, E: Purple. (Bottom) 2nd scenario: the putative leaders transmit only their current speeds in each time step; vehicles: A: Blue, B: Green, C: Red, D: Light Blue, E: Purple.

In a second example, the same simulation was performed, considering now that the putative leaders cannot transmit T and v_e but only their current speed and position. The following vehicles predict the values T and v_e, based on the naïve assumption of constant speed for their putative leaders, and continuously re-estimate those values in each time step of the MPC scheme, as described in a previous section. The corresponding simulation results are depicted in Figure 6 (Bottom). Similarly to the previous example, the system successfully executes the merging tasks in the correct order. Additionally, the vehicles manage to proceed to the downstream section with the correct speed and headway, although the assumption of constant speed was not close to the real situation. This success is attributed to the use of the MPC controller (in combination with the optimal trajectory specification), which successfully compensates for the resulting errors. However, compared to the previous example, higher values for jerk and acceleration are observed. This is expected, since the actions of the controller are based on an incorrect assumption, and, as the vehicles approach the merging point, less time is available to correct this error. Nevertheless, the application of the proposed methodology for a set of vehicles proved to be applicable and effective, while its extension to any number of interacting vehicles is straightforward.

4. CONCLUSIONS

In (*12*), a trajectory planning methodology for the facilitation of an automated merging procedure was proposed, based on the analytical solution of an optimal control problem. Only two input values from the vehicle's putative leader are needed to compute the optimal trajectory, namely the time to the merging point and the final speed at the same position. Since an accurate estimation of these input values is not possible in real situations, that methodology is applied in this paper through a MPC scheme, which compensates for possible errors. In the case that the putative leader cannot transmit the necessary values to its follower, its current speed and position can be used instead, along with a prediction of its future speed; then, the MPC scheme is used to continuously update the optimal trajectory, based on the updated values provided by the putative leader.

The simulation results demonstrate the applicability and effectiveness of the methodology, and highlight the importance of having a reasonably correct estimation for the input values. The impact of the control step length for the MPC scheme was also studied. The proposed MPC scheme for a pair of vehicles was finally extended and applied to an arbitrary set of vehicles within the cooperation area, with a prescribed merging sequence. The extended methodology includes the use of an ACC controller for all vehicles, while the MPC is used alongside the ACC inside the cooperation area. Simulation results demonstrate the applicability and effectiveness of the proposed methodology, and its potential for real-world application. Additional tests will be carried out to assess the performance of the proposed methodology in different flow conditions. Moreover, the combination of the proposed methodology with a proper upper-level controller, which delivers the merging sequence, is under development.

ACKNOWLEDGEMENTS

The research leading to these results has received funding from the European Research Council under the European Union's Seventh Framework Programme (FP/2007-2013) / ERC Grant Agreement n. 321132, project TRAMAN21.

REFERENCES

1. Davis, L. C. Effect of Cooperative Merging on the Synchronous Flow Phase of Traffic. *Physica A: Statistical Mechanics and its Applications*, Vol. 361, No. 2,

2006, pp. 606–618.
2. Pueboobpaphan, R., F. Liu, and B. van Arem. The Impacts of a Communication Based Merging Assistant on Traffic Flows of Manual and Equipped Vehicles at an On-Ramp Using Traffic Flow Simulation. In *Proceedings of the 13th International IEEE Conference on Intelligent Transportation Systems*, Madeira Island, Portugal, 2010, pp. 1468–1473.
3. Milanés, V., J. Godoy, J. Villagrá, and J. Pérez. Automated On-Ramp Merging System for Congested Traffic Situations. *IEEE Transactions on Intelligent Transportation Systems*, Vol. 12, No. 2, 2011, pp. 500–508.
4. Marczak, F., W. Daamen, and C. Buisson. Merging Behaviour: Empirical Comparison Between Two Sites and New Theory Development. *Transportation Research Part C*, Vol. 36, 2013, pp. 530–546.
5. Sun, J., J. Ouyang, and J. Yang. Modeling and Analysis of Merging Behavior at Expressway On-Ramp Bottlenecks. In *Transportation Research Record: Journal of the Transportation Research Board No. 2421*, Transportation Research Board of the National Academies, Washington, D.C., 2014, pp. 74–81.
6. Athans, M. A Unified Approach to the Vehicle-Merging Problem. *Transportation Research*, Vol. 3, No. 1, 1969, pp. 123–133.
7. Ntousakis, I. A., K. Porfyri, I. K. Nikolos, and M. Papageorgiou. Assessing the Impact of a Cooperative Merging System on Highway Traffic Using a Microscopic Flow Simulator. In *Proceedings of the ASME 2014 International Mechanical Engineering Conference & Exposition*, IMECE2014, Montreal, Quebec, Canada, Volume 12: Transportation Systems, 2014, Paper No. IMECE2014-39850.
8. Ran, B., S. Leight, and B. Chang. A Microscopic Simulation Model for Merging Control on a Dedicated-Lane Automated Highway System. *Transportation Research Part C*, Vol. 7, No. 6, 1999, pp. 369–388.
9. Davis, L. C. Effect of Adaptive Cruise Control Systems on Mixed Traffic Flow Near an On-Ramp. *Physica A: Statistical Mechanics and its Applications*, Vol. 379, No. 1, 2007, pp. 274–290.
10. Park, H., C. S. Bhamidipati, and B. L. Smith. Development And Evaluation of Enhanced IntelliDrive-Enabled Lane Changing Advisory Algorithm to Address Freeway Merge Conflict. In *Transportation Research Record: Journal of the Transportation Research Board, No. 2243*, Transportation Research Board of the National Academies, Washington, D.C., 2011, pp. 146-157.
11. Rios-Torres, J., A. A. Malikopoulos, and P. Pisu. Online Optimal Control of Connected Vehicles for Efficient Traffic Flow at Merging Roads. In *Proceedings of the 2015 IEEE 18th International Conference on Intelligent Transportation Systems*, Las Palmas, Gran Canaria, Spain, 2015, pp. 2432-2437.
12. Ntousakis, I. A., I. K. Nikolos, and M. Papageorgiou. Optimal Vehicle Trajectory Planning in the Context of Cooperative Merging on Highways. *Transportation Research Part C*, Vol. 71, 2016, pp. 464-488.
13. Papageorgiou, M., M. Leibold, and M. Buss. *Optimierung - Statische, dynamische, stochastische Verfahren für die Anwendung (Optimisation - Applied static, dynamic, stochastic methods),* 3rd Edition (revised and updated), Springer, Berlin, 2012.
14. Mattingley, J., Y. Wang, and S. Boyd. Recending Horizon Control, Automatic Generation of High-Speed Solvers. *IEEE Control Systems Magazine*, Vol. 31, No.

3, 2011, pp. 52-65.

15. Marinaki, M., and M. Papageorgiou. *Optimal Real-time Control of Sewer Networks*. Springer-Verlag, London, 2005.
16. Ntousakis, I. A., I. K. Nikolos, and M. Papageorgiou. On Microscopic Modelling of Adaptive Cruise Control Systems. In *Transportation Research Procedia*, Vol. 6, 2014, pp. 111-127.
17. Schmidt, G., and B. Posch. Automatische Zusammmenführung zweier Fahrzeugströme – eine Rückblende. *Automatisierungstechnik*, Vol. 58, No. 6, 2010, pp. 317-321.
18. Liang, C.-Y., and H. Peng. Optimal Adaptive Cruise Control with Guaranteed String Stability. *Vehicle System Dynamics: International Journal of Vehicle Mechanics and Mobility*, Vol. 32, No. 4-5, 1999, pp. 313–330.